Central Review of Amyloid-Related Imaging Abnormalities in 2 Phase 3 Clinical Trials of Bapineuzumab in Mild-To-Moderate Alzheimer's Disease Patients

Nzeera Ketter[1*], H Robert Brashear[1], Jianing Di[1,] Jennifer Bogert[2], Yves Miaux[3], Achim Gass[3], Derk D. Purcell[3], Frederik Barkhof[4], H Michael Arrighi[1],

[1]Janssen Alzheimer Immunotherapy Research & Development, LLC, South San Francisco, California 94080
[2]Janssen Research & Development, LLC, Raritan, NJ, USA
[3]BioClinica Inc., Newtown, Pennsylvania 18940 (formerly Synarc)
[4]Department of Radiology, VU University Medical Center, Amsterdam, Netherlands

***Corresponding author**:
Dr. Nzeera Ketter
Janssen Alzheimer Immunotherapy Research & Development
700 Gateway Boulevard., South San Francisco
California 94080
Tel: 510 248 2708
Fax: 510 248 2560
Email: nketter@janimm.com

Study Support: Funded by Janssen Alzheimer Immunotherapy Research & Development, LLC, and Pfizer Inc. The sponsor also provided a formal review of this manuscript.

Registration: NCT00574132 (Bapineuzumab-301), NCT00575055 (Bapineuzumab-302)

Key Words: Alzheimer's disease, Bapineuzumab, MRI, Brain Amyloid-Related Imaging Abnormality with Edema or Effusion

Running Head: Central Review of Bapineuzumab ARIA in Brain MRI Scans

Conflict of interest/disclosures:

Nzeera Ketter, H Robert Brashear, H Michael Arrighi, Jianing Di are employees of Janssen Alzheimer Immunotherapy Research & Development, LLC and all own stock/stock options in the company. Jennifer Bogert is an employee of Janssen Research & Development LLC and owns stock/stock options in the company. Yves Miaux, and Derk D. Purcell are former consultants for BioClinica (formerly Synarc), Achim Gass is an employee of University Hospital Mannheim (formerly BioClinica), and Frederik Barkhof is an employee of VU University Medical Center, Amsterdam and a former consultant to Janssen Alzheimer Immunotherapy Research & Development, LLC and all declare no conflict of interest.

All authors met ICMJE criteria and all those who fulfilled those criteria are listed as authors. All authors had access to the study data, provided direction and comments on the manuscript, made the final decision about where to publish these data and approved the final draft and submission to this journal.

Drs. Ketter, Brashear, Arrighi, and Barkhof contributed to study design and were responsible for data interpretation. Drs. Miaux, Purcell, and Gass executed, and interpreted central final read of brain MRI scans, and Ms. Bogert and Dr. Di were the project biostatisticians.

ABSTRACT (250/250 words)

INTRODUCTION: Amyloid-related imaging abnormalities (ARIA) consist of ARIA-E (with effusion or edema) and ARIA-H (hemosiderin deposits, HDs). To address challenges with real-time ARIA identification during two Phase 3 trials of bapineuzumab IV in mild-to-moderate Alzheimer's disease patients (APOE ε4 allele carriers or noncarriers), a Final Read was performed.

METHODS: Final magnetic resonance imaging (MRI) Central review consisted of a systematic, sequential locked, adjudicated read in 1,331 APOE ε4 noncarriers and 1,121 carriers by independent neuroradiologists. Assessment of ARIA-E, ARIA-H, intracerebral hemorrhages, and age-related white matter changes (ARWMC) is described.

RESULTS: In Final Read, treatment-emergent ARIA-E was identified in 242 patients including 76 additional cases not identified previously in Safety Read. Overall, incidence proportion of ARIA-E was higher in APOE ε4 carriers (active 21.2%; placebo 1.1%) than in noncarriers (pooled active 11.3%; placebo 0.6%), and was more often identified in homozygote APOE ε4 carriers than heterozygotes (34.5% vs. 16.9%). Incidence rate of ARIA-E increased with dose in noncarriers. Frequency of ARIA-E first episodes was higher after the first bapineuzumab infusion and declined after repeated infusions. Incidence of total HDs <10 mm (cerebral microhemorrhages) was higher in active groups versus placebo.

DISCUSSION: ARIA was detected more often on MRI scans when neuroradiologists were trained and results adjudicated. There was increased risk of ARIA-E in those who had HDs at baseline, and ARIA-E was a risk factor for incident ARIA-H. Treatment-emergent ARIA-E occurred early in the course of therapy and late onset ARIA-E was milder radiologically. Bapineuzumab did not influence development of ARWMC.

1. INTRODUCTION

Prominent pathological features of Alzheimer's disease (AD) are accumulation of fibrillar amyloid beta (Aβ) peptide aggregates in neuritic plaques and cerebral vasculature (amyloid angiopathy) as well as intraneuronal neurofibrillary tangles, neuritic dystrophy and synaptic loss [1, 2]. Amyloid cascade hypothesis postulates that the deposition of the amyloid-β peptide in the brain parenchyma initiates a sequence of events that ultimately lead to AD dementia. It suggests that anti-Aβ therapy may degrade or slow aggregate formation and accumulation, and enhance clearance of Aβ oligomers and aggregates resulting in reduced neurotoxicity [2, 3].

Bapineuzumab is a recombinant humanized monoclonal antibody that targets amyloid beta, $A\beta_{1-40/42}$ [4, 5]. Clinical studies of bapineuzumab and several clinical trials of therapies directed at lowering the fibrillar cerebral Aβ burden in AD were associated with findings on magnetic resonance imaging (MRI) abnormalities [6-8]. These amyloid-related imaging abnormalities (ARIA) were of two types: a) ARIA-E, parenchymal and/or sulcal hyperintensities seen on fluid-attenuation inversion recovery (FLAIR) MRI scans consistent with edema or sulcal effusion (extravasated proteinaceous fluid in leptomeninges and sulcal space), in some cases associated gyral swelling [8]; and b) ARIA-H, foci of signal void on T2*-weighted gradient- echo (GRE) brain MRI pulse sequences [9] due to magnetic susceptibility effects of hemosiderin. Extravasated fluid containing sufficient numbers of erythrocytes leads to hemosiderin deposition in the parenchyma or over the cerebral surface. ARIA-H may present as small, <10-mm punctate lesions (small hemosiderin deposits (HDs) or microhemorrhages (mHs)), or as larger, ≥10-mm linear areas of hemosiderin deposition. Small HDs (<10 mm), mHs and cerebral microbleeds are

commonly used in literature and are nearly synonymous and at times used interchangeably in this report.

Cerebral microhemorrhages are more common in AD patients than in the general population and appear to be associated with amyloid deposition. The appearance of ARIA-H is a known complication of small vessel angiopathy and cerebral amyloid angiopathy (CAA) [10]. Asymptomatic Aβ deposition in older adults was associated with lobar (posterior) microhemorrhage. Cerebral microhemorrhages occur spontaneously in up to 19% of normal elderly people [11] up to 32% of AD patients, and in 38% of patients with mild cognitive impairment [11, 12]. Incident ARIA-H was detected in 26 bapineuzumab-treated mild-to-moderate AD patients in Phase 2 studies (12.4%, 26/210). Of those with incident ARIA-H, 24 had incident microhemorrhages and two had incident large superficial hemosiderin deposits [6].

ARIA-E has been observed uncommonly in untreated patients with AD in large cohorts screened for AD clinical trials with anti-amyloid agents [13]. ARIA is likely to represent increased permeability of the blood-brain-barrier that is also observed in spontaneously occurring cerebral amyloid angiopathy.

In Phase 2 clinical studies of bapineuzumab, ARIA-E was identified in 17% (36 of 210 participants) of participants, and an increased risk observed with both increasing bapineuzumab dose and APOEε4 copy number [7, 14, 15]. It was observed in only 1% of patients on baseline MRI. A post hoc review revealed that 42% (15/36) of the ARIA-E cases in the bapineuzumab Phase 2 studies were only detected during the MRI re-read central review and missed by local

clinical site readers [7]. However, the majority of participants that developed ARIA-E during treatment did not report any associated clinical symptoms.

During the conduct of bapineuzumab Phase 3 studies in Alzheimer's patients with mild-to-moderate dementia [16], safety MRI scans were obtained following drug infusions and were read by local site radiologists. Central reading by neuroradiologists was introduced later in the study but not all scans were centrally read. However, to address challenges with the identification of ARIA-E by local readers, partly due to it being a new phenomenon it became necessary to monitor for MRI abnormalities at increasing level of detail. This study describes the process and results of a final central assessment of ARIA-E, ARIA-H, and other MRI findings using a standardized, sequential locked read methodology in two Phase 3 studies of bapineuzumab.

2. MATERIALS AND METHODS

2.1 Study population

This central MRI review was performed in patients who had completed their participation in the two Phase 3 studies as described in Salloway et al.[16] and had received at least part of one dose of bapineuzumab or placebo, and had at least one post baseline interpretable MRI.

2.2 Study design

The studies have been described previously and registered at ClinicalTrials.gov: (NCT00574132; NCT00575055) [16]. These two Phase 3 multicenter, randomized, double-blind, placebo controlled, parallel-group, efficacy and safety trials of intravenous bapineuzumab in patients

with mild-to-moderate AD who are APOE ε4 allele carriers or noncarriers. MRI exclusion criteria were two or more microhemorrhages, prior hemorrhage ≥ 1 cm^3, two or more lacunar infarcts, a prior infarct ≥ 1 cm^3 or a space-occupying lesion. According to the protocol, occurrence of ARIA-E required interruption of dosing. Participants had the option of redosing at a lower dose after resolution.

Safety MRI scans were performed at the screening visit (baseline), and 6 weeks after each bapineuzumab infusion at weeks 6, 19, 32, 45, 58, and 71. Real-time centralized reading of these MRI scans (the "Safety Read") was instituted in steps during the course of the trial. Prior to the end of trials, a second blinded central reading of all MRI scans (the "Final Read") was performed to ensure that all scans were reviewed using standardized criteria and assessed by experienced neuroradiologists trained specifically to evaluate ARIA. The Final Read was performed by a separate independent team of neuroradiologists that were blinded to the participant's clinical history and treatment group and did not communicate or discuss results with the neuroradiologists who performed the initial Safety Read. The majority of brain MRI exams were acquired on high magnetic field strength MR units (1.5 or 3 Tesla), a few exams (<10%) were acquired using 0.5 or 1.0 Tesla MR units. All MRIs were acquired using a uniform scanning protocol. A summary of MRI acquisition parameters for the main MRI scanner models at 1.5 Tesla is shown in Table 1S.

2.3 Final MRI Read process

MRI scans of all participants who received at least a partial dose of study drug were included in the Final Read. After each participant had completed trial participation, the Final Read of all interpretable scans was performed centrally by five pairs of independent neuroradiologists who were trained to recognize and quantify the extent and location of ARIA-E and ARIA-H, ARWMC, and other MRI findings. Each neuroradiologist pair, blinded to the participant's clinical history and treatment assignment, individually reviewed a patient's series of MRI scans using a sequential locked process (Figure 1). Each member of a pair of neuroradiologists independently read in sequence the patient's MRI exams displayed on the same type of reading station (BioClinica, Table 1S).

Individual neuroradiologist reader assessments for each sequential scan were reported on standardized electronic case report forms and their initial assessment was locked. After reviewing the next sequential scan, modifications to the initial assessment were permitted, then that modified form was locked and was considered the final retrospective MRI assessment. Thus for each MRI scan, the reviewer's initial and final assessments were recorded. Discrepancies between the final assessments within each pair of neuroradiologist were discussed amongst themselves using prespecified rules shown in Figures 2S and 3S of supplemental section to obtain a consensus score. Consensus results were analyzed to estimate the baseline prevalence and incidence and severity of MRI findings.

The location and the largest cross-sectional diameter of abnormal parenchymal hyperintensity, sulcal hyperintensity and gyral swelling were measured on FLAIR MRI sequences for each of six brain regions per hemisphere (frontal, temporal, parietal, occipital, cerebellum/brainstem, and central [hypothalamus, pons, basal ganglia]). For this study, an ARIA–E event was considered treatment-emergent if it started during or after the first infusion of bapineuzumab and on or before 137 days prior to the last dose. Duration of ARIA-E was defined as the time from first detection on MRI scans until complete resolution. A radiologic severity score of 0 to 5 was given based on spatial extent and multifocality of the abnormality within each region and a total maximum score was obtained by summing across the 12 regional scores (range of total score 0-60) [17].

The number of definite or possible small HDs (mHs), and large HDs, detected as foci of decreased signal on T2*-weighted gradient recalled echo (GRE) MRI sequence, was recorded for each brain region. New HDs <10 mm and ≥10 mm in size were assessed by anatomical region and adjudicated for number and size, and total numbers were derived. Parenchymal hemorrhage >1 cm in size was adjudicated by presence/absence and size.

Age-related white matter hyperintensities (ARWMC), ≥ 5 mm were scored on FLAIR images, [18]. They were adjudicated by presence/absence for left and right hemispheres frontal, parieto-occipital, temporal, basal ganglia, and infratentorial/cerebellum regions. The total score was the sum of ARWMC rating scale scores for white matter and basal ganglia lesions in each region. In addition, other potentially relevant MRI findings were recorded by location, size, and description

(eg, infarct, encephalomalacia, aneurism, arteriovenous malformation, subdural hematoma, space-occupying lesion, hydrocephalus, and other).

The objectives of the MRI Final Read were as follows: 1) to characterize ARIA-E incidence proportion, radiologic severity, and the temporal relationship between study drug infusion and occurrence of ARIA-E; 2) to estimate the prevalence of small HDs (<10 mm, microhemorrhages) and larger HDs (≥10 mm, mainly linear areas) at screening, their incidences over time, and their relationship to study drug infusion; 3) to characterize the relationship of incident HDs with ARIA-E; and 4) to estimate the incidence of cerebral infarcts and lobar hemorrhages.

2.4 Statistical analysis

Study data were summarized over time by treatment arm using summary statistics. Incidence proportions were calculated as the ratio of the number of participants with the event to the total number of participants in the study population times 100. The exact binomial 95% CI was calculated for event incidence proportions within each treatment group and for the difference between each bapineuzumab group and placebo. The Poisson exact 95% CI was calculated for each treatment group incidence rate and for the difference in incidence rates between each bapineuzumab group and placebo. The incidence rate per 100 person-years was calculated as $\lambda = Y/t \times 100$, where Y is the number of participants who had the event at least once during the exposure period and t is the total person-years at risk.

In addition, time to first ARIA-E occurrence was analyzed using the Kaplan-Meier method. The incidence proportion of participants with first episode of treatment-emergent ARIA-E by number

of infusion received was analyzed using binomial 95% CI; events of dosed-through ARIA-E were also summarized.

Inter-reader agreement/reliability (κ) and the intraclass correlation coefficient (ICC) by scan for each reader pair were determined [19]. The ICCs and their 95% confidence intervals were calculated using the SAS ICC9 Macro code [20]. All analyzes were performed by using SAS Statistical software (SAS institute, Cary NC).

3. RESULTS

3.1 Population

Participant baseline characteristics and disposition were previously described by Salloway et al. [16]. A total of 9,310 MRI scans were reviewed in 1,331 APOE ε4 noncarriers that were from 524 patients on placebo and from 337, 329 and 141 patients on bapineuzumab 0.5, 1.0, and 2.0 mg/kg doses respectively. Similarly, 7,840 scans were reviewed in 1,121 APOE ε4 carriers of which 448 were on placebo and 673 were on bapineuzumab 0.5 mg/kg.

3.2 Safety Read versus Final Read

Treatment-emergent ARIA-E was identified in 242 participants (148 APOE ε4 carrier and 94 APOE ε4 noncarrier participants). The MRI Final Read detected 76 additional cases (31%) that were not identified by the central Safety Read during the study (Table 1). ARIA-E that was only detected in the Final Read was either captured on MRIs that were not read during the Safety Read (33% [25/76]) or was missed (67% [51/76]) because the findings were minimal or subtle

(Table 1). The majority of missed Safety Read ARIA-E cases (88% [45/51]) had a radiological severity score ≤2 and only 10% (5/51) had severity score ≥3. Approximately 80% of the ARIA-E cases of the entire pool had both parenchymal and sulcal hyperintensity on MRI scans. Four ARIA-E cases that were identified in Safety Read but not in the Final Read included three that were downgraded as not ARIA-E or not treatment-emergent and one was not recognized in the Final Read. In one case of ARIA-E detected by Safety Read the scan was not available to Final Read for verification.

Treatment-emergent cerebral hemorrhage with ARIA-E was noted in 2 participants (one in each 0.5 and 1.0 mg/kg bapineuzumab noncarrier groups) in the Final Read that was not recognized in the Safety Read. ARIA-E in participant in the 0.5 mg/kg group was associated with a TEAE of parenchymal left occipital hemorrhage. Participant in 1.0 mg/kg group with ARIA-E also had cerebral hemorrhage reported as TEAE that occurred after the final MRI scan visit.

A comparison of MRI scan visit start dates when ARIA-E episode were first detected in the Final and Safety Reads, showed that of the 165 total ARIA-E cases detected among carriers and noncarriers, 40 cases (12 in noncarriers, and 28 in carriers) were detected first in the Final Read as compared to only four cases (2 in each noncarrier and carriers) first detected in the Safety Read, and 121 cases had the same detection date. Detection of earlier first onset of ARIA-E in the Final Read is expected as central neuroradiologists who had more experience with ARIA-E had reviewed earlier scans for suspicious cases. Similarly, ARIA-E duration in the Final and Safety Reads were compared by visit dates at which ARIA-E was no longer present (i.e. stop dates). The duration of ARIA-E was measured as longer in the Final Read for 86 of the 165 cases, longer in the Safety Read for 22 cases and as having the same duration in 57 cases. There

were six participants for whom two ARIA-E episodes reported in the Safety Read in the same individual actually comprised a single long, evolving episode in the Final Read. For 4 participants there was one long ARIA-E episode in the Safety Read which was shown to be two independent episodes in the Final Read.

Concordance and discordance between reader pairs indicated that the overall agreement within each pair of neuroradiologists prior to consensus adjudication was high with kappa coefficient values of 0.73 for the presence of ARIA-E, and 0.69 for the presence of ARIA-H <10 mm. In addition, the ICC by scan for each reader pair for ARIA-E total score was 0.90 (95% CI: 0.89, 0.90); for ARIA-H <10 mm, total count was 0.92 (95% CI: 0.91, 0.92), and for white matter hyperintensity total score was 0.89 (95% CI: 0.88, 0.89). Actual examples of ARIA-E adjudication where there was a change before and after adjudication from the same pair of readers included one MRI in which one reader's Final Read did not detect any hyperintensity whereas the other reader identified parenchymal hyperintensity with a score of two in both right parietal (RP) and right occipital (RO) locations. The final adjudicated result had no parenchymal hyperintensity where reader 1's observation prevailed. Another example from the same pair of readers indicated that reader 1's Final Read observed evidence of parenchymal hyperintensity in the RP and RO locations with scores of three for each, but the reader 2's Final Read did not and the adjudicated findings was parenchymal hyperintensity with scores of three in two regions where reader 2's observation had prevailed.

3.3 ARIA-E incidence (Final Read), severity score and temporal relationships

3.3.1 ARIA-E incidence

ARIA-E Final Read incidence proportion and incidence rate per 100 person-years for each treatment group and the difference between bapineuzumab and placebo groups are summarized in Table 2. The incidence proportion of ARIA-E increased with dose in noncarriers (Figure 2). Based on the Final Read in the noncarrier study, the incidence proportion (95% CI) of treatment-emergent ARIA-E were 5.6% (3.4, 8.7), 13.4% (9.9, 17.5) and 19.9% (13.6, 27.4) for bapineuzumab 0.5mg/kg, 1.0 mg/kg and 2.0 mg/kg groups respectively compared with 0.6% (0.1, 1.7) in the placebo group. Treatment-emergent incidence proportion (95% CI) of ARIA-E in carriers were 21.2 % (18.2, 24.5) in the 0.5 mg/kg group versus 1.1% (0.4, 2.6) in the placebo group and was more often identified in homozygote APOE ε4 carriers than heterozygotes (34.5%, vs. 16.9%, Table 2). At the same 0.5 mg/kg bapineuzumab dose, incidence proportion of ARIA-E was highest in carriers of two copies of APOE ε4 allele (34.5%, 95% CI: 27.3, 42.3) as compared to noncarriers (5.6%, 95% CI: 3.4, 8.7), and carriers with one copy of the allele (16.9%, 95% CI: 13.8, 20.5) (Figure 2). In participants from the two studies who received the same dose of bapineuzumab, the incidence rate of ARIA-E and its difference from placebo were higher in carriers than in noncarriers (20.7 vs. 5.0; and 19.7 vs. 4.5 respectively; see Table 2). In homozygote APOE ε4 carriers, the incidence rate of ARIA-E and its difference from placebo was higher than in those with one copy of the allele (Table 2).

3.3.2 ARIA-E radiological severity scores

Table 3 shows the total mean maximum radiological severity score as determined by the highest total score within a series of MRI scans for first episode of an ARIA–E event for all treatment groups. In noncarriers, the mean maximum total radiological severity score of ARIA-E was higher in bapineuzumab treatment groups than in placebo group with no evidence of a clear dose-response. [8.9 (1 to 46), 6.3 (1 to 56), and 9.9 (1 to 57) in the 0.5, 1.0, and 2.0 mg/kg groups, respectively; placebo, 4 (range 2 to 7)] There was a trend in lower mean maximum severity scores in later infusions across the three bapineuzumab dose groups and higher scores with higher dose in two earlier infusions. In carriers, the corresponding mean maximum total radiological severity score was higher in the 0.5 mg/kg group (12.3 [1 to 61]) compared to the placebo group (2.0[1 to 4]). The total maximum scores of the first occurrence of ARIA-E were lower for different patients with later onsets of ARIA-E after longer initial exposures to bapineuzumab. The mean scores of first ARIA-E episode in carriers after the first, second, third, fourth, fifth, and sixth infusions were 8.3, 8.6, 6.1, 2.9, 5.7, and 5.0, respectively.

3.3.3 Temporal relationships

Occurrences of first episodes of treatment-emergent ARIA-E incidence by bapineuzumab infusion number are summarized in Table 3. In both carriers and noncarriers, first ARIA-E episode occurred early during the course of treatment with a higher frequency occurring after the first infusion, and declining after repeated infusions, illustrated in Figure 3. In noncarriers, the incidence of first occurrence of treatment-emergent ARIA-E detected by the MRI Final Read was higher during the interval between the first and third infusions of bapineuzumab as

compared to subsequent infusions. In the bapineuzumab 0.5 and 1.0 mg/kg groups, the incidence proportions were 1.5%, 7.0% between the first and second infusions compared to 2.5% and 4.5% respectively between the second and third infusions. In the bapineuzumab 2.0-mg/kg group, the incidence of initial cases of treatment-emergent ARIA-E was highest after the first infusion (12.1%), when approximately 60% of patients in this group with ARIA-E (17/28) had this event. In the placebo group, three single cases of ARIA-E occurred after the first, second and fourth infusions.

In carriers, 84.6% (121/143) of first episode of ARIA-E occurred between the first and fourth bapineuzumab infusions (week 0 to 39) relative to subsequent infusions. In the bapineuzumab group, the incidence proportions of initial cases of treatment-emergent ARIA-E were 5.8% between the first and second infusions, 9.0% between the second and third infusions, and 4.2% between the third and fourth infusions (Table 3). In the placebo group, the incidence of initial cases of ARIA-E occurring after the first, third, and sixth infusions was 0.4%, 0.5%, and 0.3%, respectively. The incidence proportion of the first episode of an ARIA-E event was higher in bapineuzumab-treated APOE ε4 carriers than in noncarriers at the same dose level (0.5 mg/kg) for the first three infusions.

The median time to first occurrence of ARIA-E and the Kaplan-Meier estimates of the distribution of treatment-emergent ARIA-E among different treatment groups is shown in Table 4. In general, the first episode of ARIA-E was more spread out across all drug infusions in carriers than noncarriers. In noncarriers, first episode of ARIA-E occurred earlier as the dose of

bapineuzumab increased and the KM 10th percentile (95% CI) of the time to first occurrence of ARIA-E was shorter for the 2.0 mg/kg dose group [45 (41, 134) days] as compared to 1.0 mg/kg group [135 (48, 316) days]. In carriers, the median time to first ARIA-E occurrence was 134 days and 225 days for the bapineuzumab and placebo groups, respectively, and the Kaplan-Meier estimate of the 10th percentile of the time to first occurrence of ARIA-E was 133 days (95% CI, 131, 135 days) for the bapineuzumab group. The estimated number of days to first occurrence is influenced, in part, by the frequency of MRI scans, a mean of every 91 days.

In noncarriers, across all treatment groups, the majority of ARIA-E events 74% (70/94) identified in the MRI Final Read resolved by the end of study (Table 4). Median duration of resolved cases decreased with higher dose. Twenty-four participants had ARIA-E events that had not resolved by the end of the study (9, 7, and 8 in the bapineuzumab 0.5-, 1.0-, and 2.0-mg/kg groups, respectively [0 in placebo group]). These ARIA-E occurrences were late-occurring events for which there was no subsequent MRI scan. In bapineuzumab-treated carrier group, the majority of ARIA-E resolved cases [81.1% (116/143)] had a median duration of 129 days (Table 4).

3.3.4 Dosing-Through ARIA-E

Noncarriers with treatment-emergent ARIA-E who were not recognized in the Safety Read (49 of the 94 participants ~ 52%) continued to receive drug during an episode. Total maximum mean ARIA-E radiological severity scores (parenchymal, sulcal edema or effusion plus gyral swelling) were similar for participants who continued to receive drug during ARIA-E episodes

compared to those who were discontinued in the bapineuzumab 1.0 and 2.0 mg/kg groups (11.2 vs. 10.1; 17.8 vs. 20.3 respectively) but were higher for those who were dosed-through in the 0.5 mg/kg group (18.6 vs. 8.9).

Overall, in all bapineuzumab groups, the median duration of ARIA-E episodes (resolved and unresolved) was shorter for participants who stopped receiving drug (365, 93, 99 and 44 days for 0.5, 1.0, and 2.0 mg/kg and placebo groups respectively) as compared to those that were dosed-through (230, 183, 176 and 143 days for bapineuzumab and placebo groups respectively). While this difference in duration is likely influenced by differences in MRI scan schedule with more frequently-timed follow up MRI scans in the not dosed-through cohort compared to the dosed-through cohort, this would account for only about a 30-day bias due the protocol requirement for a shorter interval (approximately every 4 weeks) between MRI scans once ARIA-E was recognized. As the difference in median duration of resolved ARIA-E cases was approximately 90 days in all bapineuzumab groups, this suggests that additional factors contribute to this effect.

In carriers, 91 participants in the bapineuzumab group were dosed-through during ARIA-E event and 52 were not. Radiological severity score for participants in the bapineuzumab group that were dosed-through was comparable to all ARIA-E cases. The median duration of resolved ARIA-E episodes was longer, (182 days (range 78, 457)) for those who were dosed-through an episode as compared to those not dosed-through (96.0 days (range 32, 302).

Of the 65 noncarriers on bapineuzumab who had an initial episode of ARIA-E in the Safety Read, 39 participants (60%) re-initiated bapineuzumab infusions after their ARIA-E episode had resolved. Recurrent episodes of ARIA-E occurred in 10 of these 39 participants across the bapineuzumab groups, including nine which recurred after re-initiation of treatment (1, 4, and 4 in the 0.5, 1.0, and 2.0-mg/kg groups, respectively) and 1 in 0.5 mg/kg group which recurred spontaneously off treatment. Similarly, of the 103 carriers on bapineuzumab with ARIA-E 50 resumed bapineuzumab infusions after ARIA-E episode resolved; 11 had a recurrence of ARIA-E after re-initiation of treatment and two occurred spontaneously without being re-dosed.

3.4 ARIA-H incidence (Final Read) and temporal relationships

3.4.1 Hemosiderin deposits <10 mm

For the two bapineuzumab studies, MRI exclusion criteria were two or more microhemorrhages or prior hemorrhage ≥ 1 cm^3. The baseline prevalence (95% CI) of total (definite or possible) HDs <10 mm for carrier and noncarrier participants with and without treatment-emergent ARIA-E identified in the MRI Final Read is shown in Table 5. Approximately 13% to 19% of participants in all treatment groups had HD <10mm at baseline. In noncarriers, the prevalence of participants with total (definite or possible) HDs<10 mm at baseline was similar for the placebo (16.6% (13.5, 20.1)) and 0.5 mg/kg (13.4% (9.9, 17.5)) and 1.0 mg/kg (15.8% (12.0, 20.2)) bapineuzumab groups but was slightly higher in the 2.0 mg/kg group (19.1% (13.0, 26.6)). There was no cerebral regional preponderance for the development of HDs <10 mm. In carriers, the incidence proportion of total (definite or possible) HDs <10 mm at baseline was similar between the placebo (16.7% (13.4, 20.5)) and 0.5 mg/kg group (17.8% (15.0, 20.9)).

In noncarriers, the frequency of treatment-emergent ARIA-E was higher among participants that had HDs <10 mm (mHs) at baseline than those without HDs for the 0.5-mg/kg group (6.7% [3/45] vs. 5.5% [16/292]) and for the 2.0-mg/kg group (25.9% [7/27] vs. 18.4% [21/114]), but not for the 1.0-mg/kg group (11.5% [6/52] vs. 13.7% [38/277]). In the bapineuzumab 2.0 mg/kg group, the mean number (range) of incident (definite or possible) HDs <10 mm identified on the MRI Final Read was higher in scans during the treatment-emergent ARIA-E episode relative to the incident number on scans taken at onset of ARIA-E [5.5 (-17, 100) vs. 1.2 (-1, 6)]. The same trend though less pronounced was observed in the 1.0 mg/kg group [1.7 (-2, 19) vs 0.8 (0, 10)]. A negative number of HDs represent a decrease from previous measurement. The occurrence of incident HDs <10 mm after resolution of the ARIA-E episode in the 2.0 mg/kg group decreased relative to the previous measurement (mean, -0.4). After each infusion, the mean number of incident HDs<10 mm and the proportion of participants with none or one HDs <10 mm were similar for those treated with bapineuzumab who were and were not dosed-through an ARIA-E episode.

In carriers, among participants with total HDs<10 mm at baseline a greater proportion of participants (95% CI), had treatment-emergent ARIA-E than those without HDs in the placebo [2.7% (0.3, 9.3) vs. 0.8 (0.2, 2.3)] and bapineuzumab groups [31.7% (23.5, 40.8) vs.19.0% (15.8, 22.5)]. Also, the mean number of new total HD <10 mm during an ARIA-E episode [4.2 (range -30, 117)] was higher relative to the incident number on scans at onset of ARIA-E episode [1.4 (-2, 21)].

The total incidence proportion (95% CI) of treatment-emergent HDs <10 mm in noncarriers was 21.4 % (17.9, 25.1) in the placebo group, and, 24.9% (20.4, 29.9), 28.0 (23.2, 33.1) and 28.4% (21.1, 36.6) in bapineuzumab 0.5, 1.0, and 2.0 mg/kg dose groups respectively. The corresponding incidence proportion of total treatment-emergent HDs <10 mm in carriers was 24.3% (20.4, 28.6) in the placebo group and 32.7% (29.2%, 36.4) in the 0.5 mg/kg dose group.

In noncarriers, the proportion of participants with ARIA-E who had their first treatment-emergent HD(s) <10 mm was highest after the first infusion than after subsequent infusions shown in Table 6. The participants in the placebo group that had ARIA-E had no treatment-emergent HDs <10 mm. The mean number of HDs <10 mm, as well as the proportion of participants having none or one HDs, after each infusion was similar for bapineuzumab 0.5- and 1.0-mg/kg groups who were or were not dosed-through an ARIA-E episode. In the bapineuzumab 2.0-mg/kg group, however, participants who were dosed-through had a greater mean number of incident HDs <10 mm after the first and second infusion than subsequently.

In carriers, the same trend was observed in which the highest incidence proportion of first episode of treatment-emergent HDs<10 mm occurred following the second infusion of bapineuzumab. The participants in the placebo group that had ARIA-E had no treatment-emergent HDs <10 mm. In the bapineuzumab group, the mean number of HDs <10 mm and the proportion of participants having none or one HDs <10 mm after each infusion was similar for those that were and were not dosed-through an ARIA-E episode.

3.4.2 Hemosiderin deposits >10 mm

Large HDs ≥10 mm were excluded at screening and therefore its baseline prevalence was low (0.18% in carriers and noncarriers). In noncarriers, incidence proportions (95% CI) of treatment-emergent HDs ≥10 mm was 1.3% (0.5,2.7) in the placebo group and 2.1% (0.8, 4.2) and 3.3% (1.7, 5.9) in the 0.5 and 1.0 mg/kg dose groups respectively. In each bapineuzumab group, the highest incidence proportion by infusion interval occurred following the first infusion. There were 7 and 3 participants in 1.0 and 0.5 mg/kg groups respectively with treatment-emergent ARIA-E and first episode of HDs ≥10 mm. In carriers, the corresponding incidence (95% CI) of treatment-emergent HDs ≥10 mm was 2.7% (1.4% to 4.6%) and 6.4% (4.7% to 8.5%) in the placebo and 0.5 mg/kg groups respectively. The highest incidence proportion of participants with a first episode of treatment-emergent HDs ≥10 mm occurred following the second infusion (1.7%). Similarly, the highest incidence proportion of participants with ARIA-E who had a first episode of treatment-emergent HDs ≥10 mm occurred following the second infusion (7.4%).

3.5 Incidence of age-related white matter change (ARWMC), and cerebral infarcts

ARWMC was not an MRI exclusion criterion and was present at baseline in 68% of carriers and 70% of noncarriers. In the placebo groups, 8% of carriers and 10% of noncarriers had a total score of >7/30 at baseline equivalent to involvement of approximately 25% of white matter (score of 3 in 4 regions) [21]. In noncarriers, there was little or no change in the mean ARWMC score from baseline to the final MRI scan in any treatment group over 18 months. In carriers, there was essentially no change in the mean ARWMC score from baseline to the final MRI scan

at end of study in either the placebo (baseline, 4.7; final scan, 4.8) or bapineuzumab 0.5 mg/kg groups (baseline, 4.5; final scan, 4.5) groups.

In noncarriers, the incidence proportion of lacunar, other, and all infarcts were low (3.8%) and similar in the bapineuzumab 0.5, 1.0 mg/kg and the placebo group. The incidence proportion (95% CI) of treatment-emergent intracranial hemorrhage was similar for the placebo (1.3% (0.5, 2.7)) and bapineuzumab 1.0 mg/kg (1.8% (0.7, 3.9)) groups, but was higher in the 2.0 mg/kg group (2.8%, n=4 (0.8, 7.1)) and lower in the 0.5 mg/kg group (0.3% (0.0, 1.6)). The mean (SD) duration of resolved intracranial hemorrhage events were 102.5 days (92.04) for the placebo group (n=6), and 38.5 days (41.32), for 1.0 mg/kg group (n=4). In the 0.5, and 2.0 mg/kg dose groups, the single intracranial hemorrhage cases resolved after 6 and 9 days respectively.

In carriers, the incidences of lacunar, other, and all infarcts were similar in the bapineuzumab (1.5%, 1.9%, and 3.3% respectively) and the placebo groups (0.7%, 1.6%, and 2.0% respectively). There was no difference in the incident proportion of treatment-emergent intracranial hemorrhage in the placebo (0.4%, n=2) and bapineuzumab groups (0.4%, n=3). In the bapineuzumab group, 2 had cerebral hemorrhage, and one had both subarachnoid hemorrhage and subdural hemorrhage, and in the placebo group, one had cerebral hemorrhage and one had subdural hemorrhage. The incident proportion of treatment-emergent subdural hematoma was 0.6% in the bapineuzumab group (n=4) and 1.1% in the placebo group (n=5). For the bapineuzumab and placebo groups, the mean (SD) duration of resolved intracranial hemorrhage was 108.3 days (92.01), and 8 days (0.0) respectively. The mean (SD) duration for the combined intracranial hemorrhage and subdural hematoma resolved events were 70.5 days (55.99) and 86.9 days (69.14) respectively.

4. DISCUSSION

Despite negative results of recent trials of several anti-Aβ immunotherapies in Alzheimer's disease, there are anti-Aβ immunotherapies in current development and there are proposals for intervention to be applied earlier in the course of AD, in prodromal and in preclinical AD [22]. Mounting evidence suggests ARIA is related to intervention in movement of amyloid from the parenchyma into the perivascular space as well as removal of vascular amyloid [16, 23]. ARIA-E (with effusion or edema) and ARIA-H (with HDs) were first reported with bapineuzumab in Phase 1 and Phase 2 clinical trials [7, 14, 15] and it was subsequently recognized that central reading improved the ascertainment rate. ARIA-E has since been associated with other amyloid–modifying therapies [24, 25]. Hence, the higher rates of ARIA-E now recognized as adverse events in patients exposed to amyloid-modifying agents.

In bapineuzumab Phase 3 studies as more ARIA was observed it became necessary to capture brain MRI abnormalities in an increased level of detail in an objective manner to improve detection and to ensure MR imaging features consistent with ARIA-E are systematically evaluated and assessed. Thus, implementation of a centralized systematic sequential locked procedure and scoring system for assessment of MRI images by experienced and trained pairs of neuroradiologists made it possible to systematically analyze ARIA cases in the MRI Final Read. Therefore, some discrepancy between the incidence proportion of ARIA-E in Safety Read while the study was ongoing and Final Read was expected. This difference was probably due to the increased experience of the readers and clinicians as the studies progressed as well as the improved Final Read process that could be key for regulators and future trial design. Ascertainment of cases improved over the course of the study due to increased familiarity and

learning curve of central Safety Readers. Of the 242 cases of ARIA-E identified in the Final Read, 76 were not detected during the study because some images for the last two visits were not read centrally (per protocol at the time) (25 cases), or because they were not identified by the central/local readers (51 cases) mainly due to low radiologic severity. Detection of ARIA-E events with more subtle radiologic appearance at an earlier stage could have consequences for patient care by allowing clinical decisions regarding dosing to be made at an earlier stage.

Somewhat higher prevalence of microhemorrhages in bapineuzumab 2.0 mg/kg participants that did not enroll as long as placebo and lower dose groups (due to discontinuation of the 2.0 mg/kg dose) suggests that microhemorrhages were more rigorously excluded later in the study, further indicating evidence of Safety Reader's learning curve. Therefore the Final Read analysis showed that Safety Readers did identify majority of occurrences of ARIA-E later in the study. The high ICC index in the Final Read indicates good agreement within pairs of neuroradiologist raters. ICC $\geq$ 0.81 is considered to indicate excellent agreement [17]. ICC values for ARIA-E total radiological severity scores, ARIA-H <10 mm total counts and white matter hyperintensity total scores were all $\geq$0.89 that indicates high degree of inter-rater reliability in assessment of these imaging abnormalities. The overall inter-reader agreement prior to consensus for ARIA-E and ARIA-H Final Read were high with kappa coefficient=0.73 and 0.69 respectively similar to that reported in literature ranging from 0.33 to 0.78 [6, 7, 26].

The incident proportion of treatment-emergent ARIA-E was higher in bapineuzumab-treated APOE*ε4 carriers (active 21.2%; placebo 1.1%) than in noncarriers (pooled active 11.3%; placebo 0.6%). The finding of higher incidence of ARIA-E with increasing bapineuzumab dose and number of APOE ε4 alleles is also consistent with Phase 2 results [7, 16]. Postmortem

studies have shown correlations between the presence of an APOE ε4 allele and amyloid-positivity in the brains of patients with sporadic AD [27].

In a ^{11}C-Pittsburg compound B (^{11}C-PiB) positron emission tomography (PET) imaging substudy of approximately 10% of enrolled participants in bapineuzumab Phase 3 trials, effects of bapineuzumab on brain Aβ burden was evaluated [28]. The imaging results demonstrated a significant reduction of fibrillar Aβ accumulation only in APOE ε4 carriers (mild AD subgroup, MMSE ≤ 21) treated with bapineuzumab as compared to placebo but not in the noncarrier mild or moderate subgroups [28]. However, the lower prevalence of significant Aβ burden in noncarriers vs carriers (63.9% amyloid positive vs.93.5%) and increased Aβ deposition among placebo participants (due to natural disease progression) may lead to an underestimation of the treatment effect. Therefore, it is possible that if differences in amyloid positivity rates in the two study cohorts are taken into account, incident rates of treatment-emergent ARIA-E may become more similar in the carrier and noncarriers.

The incidence of ARIA-E decreased as duration of exposure increased as ARIA-E tended to occur early during the course of treatment with bapineuzumab and its frequency declined after repeated infusions. There was a trend toward a shorter duration of treatment-emergent ARIA-E as the dose of bapineuzumab increased, which could be reflective of more aggressive removal of amyloid. Duration of treatment-emergent ARIA-E cases that resolved indicated a trend toward a shorter duration with increase in dose, but this may also be due to earlier onset and greater dose discontinuation at the higher doses. There were too few placebo participants with ARIA-E to

draw firm conclusions concerning potential differences in time to onset between placebo and bapineuzumab groups perhaps driven by lower recognition in placebo group with sparse follow up MRI.

Overall, discontinuation of bapineuzumab during ARIA-E episodes appeared to shorten the duration of the ARIA-E episode compared to participants who remained on study treatment during the ARIA-E episode. A possible cause of dosing through was that cases were missed because they were subtle and had low radiological scores on the Final Read.

The incidence of treatment-emergent ARIA-E was numerically higher among participants who had HDs <10 mm at baseline compared to those who did not. Incident HDs <10 mm were associated with the occurrence of ARIA-E, but there was no evidence suggesting any increase in incident HDs <10 mm once ARIA-E had resolved in any bapineuzumab group. Higher drug dose may cause more amyloid to be removed, resulting in intraparenchymal extravasation of fluid. Incident cerebral hemosiderin deposition was more common in patients treated with bapineuzumab than with placebo, and was often associated with the occurrence of ARIA-E. There was an increased risk of ARIA-E in those who had HD's at baseline. The proportion of participants with a first episode of treatment-emergent HDs <10 mm after early infusions was greater than after late infusions for the bapineuzumab group, following the same time course pattern as ARIA-E.

The total mean maximum radiological severity scores of the first occurrence of ARIA-E were lower over time across the six bapineuzumab infusions, but did not show a clear dose-related

trend. In addition to confirming the previous understanding that treatment-related ARIA-E occurs early in the course of therapy, these results demonstrate that late onset ARIA-E appears milder radiologically. The rapid early removal of amyloid in the vascular smooth muscle may be involved. Frequency of incident intracranial hemorrhage and subdural hematoma identified in the Safety Read was not notably higher in the bapineuzumab groups compared to the placebo group and Final Read confirmed only few cases not recognized in the Safety Read.

Challenges remain with specific animal models to consistently model Aβ therapy induced ARIA-E. A particular challenge following passive immunization with monoclonal antibodies with high affinity for Aβ plaques and cerebral amyloid angiopathy is increase in cerebral microhemorrhage due to weakening of blood vessel smooth muscle wall [29] and increased clearance of deposited Aβ following cerebral ischemic challenge [30]. Zago et al [23] reported on plaque-bearing PDAPP mice model immunized with murine 3D6 parent of humanized bapineuzumab to evaluate vascular alterations related to central Aβ pathology and after anti-Aβimmunotherapy. Treatment with 3D6 Aβ antibody induced clearance of vascular Aβ that was spatially associated with a transient increase in microhemorrhage and in capillary Aβ deposition. This suggested that vascular leakage events such as microhemorrhage during initial phases of Aβ clearance by immunotherapy may be due to the removal of leptomeningeal vascular Aβ but were not associated with capillaries. The transient increase in capillary Aβ accumulation after immunotherapy was likely due to reduced capacity of perivascular clearance of Aβ. Critically this work showed improved vascular integrity and reduced occurrence of microhemorrhages with continued antibody treatment.

5. CONCLUSIONS

These studies support the conclusion that it is possible and advisable to monitor centrally for ARIA. ARIA was detected more often in MRI scans in the Final Read, as neuroradiologists were trained and the results adjudicated. This study highlights that eligibility and Safety Readings should be done by trained central readers and that these abnormalities can be successfully and reliably assessed. Incidence of ARIA-E increased with increasing bapineuzumab dose and number of APOE ε4 alleles. Treatment-related ARIA-E occurs early in the course of therapy and its incidence decreased as duration of exposure increased. There appeared to be a relationship between ARIA-H and ARIA-E both probably related to underlying CAA. Microhemorrhages may cause, or be the result of, higher brain amyloid accumulation and were more common in participants treated with bapineuzumab than placebo. Microhemorrhages are often associated with ARIA-E and both radiological features are likely related to removal of vascular Aβ, although they can also be associated with the underlying disease. Bapineuzumab did not appear to influence the development ARWMC.

ACKNOWLEDGEMENTS

The authors are most grateful to the study participants for their contributions and the investigational staff for the medical care. The authors acknowledge Bradford Challis (Janssen Research & Development, LLC) for assistance in preparation and editorial support of the manuscript, and Steve Einstein (Janssen Alzheimer Immunotherapy Research & Development, LLC) for development of the independent radiological safety assessment charter and the MRI scan acquisition parameters for scanners used in the study.

REFERENCES

[1] Haass C, Selkoe DJ (2007) Soluble protein oligomers in neurodegeneration: lessons from the Alzheimer's amyloid beta-peptide. *Nat Rev Mol Cell Biol* **8**, 101-112.

[2] Hardy J, Selkoe DJ (2002) The amyloid hypothesis of Alzheimer's disease: progress and problems on the road to therapeutics. *Science* **297**, 353-356.

[3] Golde TE, Schneider LS, Koo EH (2011) Anti-abeta therapeutics in Alzheimer's disease: the need for a paradigm shift. *Neuron* **69**, 203-213.

[4] Bard F, Cannon C, Barbour R, Burke RL, Games D, Grajeda H, Guido T, Hu K, Huang J, Johnson-Wood K, Khan K, Kholodenko D, Lee M, Lieberburg I, Motter R, Nguyen M, Soriano F, Vasquez N, Weiss K, Welch B, Seubert P, Schenk D, Yednock T (2000) Peripherally administered antibodies against amyloid beta-peptide enter the central nervous system and reduce pathology in a mouse model of Alzheimer disease. *Nat Med* **6**, 916-919.

[5] Miles LA, Crespi GA, Doughty L, Parker MW (2013) Bapineuzumab captures the N-terminus of the Alzheimer's disease amyloid-beta peptide in a helical conformation. *Sci Rep* **3**, 1302.

[6] Barakos J, Sperling R, Salloway S, Jack C, Gass A, Fiebach JB, Tampieri D, Melancon D, Miaux Y, Rippon G, Black R, Lu Y, Brashear HR, Arrighi HM, Morris KA, Grundman M (2013) MR imaging features of amyloid-related imaging abnormalities. *AJNR Am J Neuroradiol* **34**, 1958-1965.

[7] Sperling R, Salloway S, Brooks DJ, Tampieri D, Barakos J, Fox NC, Raskind M, Sabbagh M, Honig LS, Porsteinsson AP, Lieberburg I, Arrighi HM, Morris KA, Lu Y, Liu E, Gregg KM, Brashear HR, Kinney GG, Black R, Grundman M (2012) Amyloid-related imaging

abnormalities in patients with Alzheimer's disease treated with bapineuzumab: a retrospective analysis. *Lancet Neurol* **11**, 241-249.

[8] Sperling RA, Jack CR, Jr., Black SE, Frosch MP, Greenberg SM, Hyman BT, Scheltens P, Carrillo MC, Thies W, Bednar MM, Black RS, Brashear HR, Grundman M, Siemers ER, Feldman HH, Schindler RJ (2011) Amyloid-related imaging abnormalities in amyloid-modifying therapeutic trials: recommendations from the Alzheimer's Association Research Roundtable Workgroup. *Alzheimers Dement* **7**, 367-385.

[9] Arrighi HM, Barakos J, Barkhof F, Tampieri D, Jack C, Jr., Melancon D, Morris K, Ketter N, Liu E, Brashear HR (2015) Amyloid-related imaging abnormalities-haemosiderin (ARIA-H) in patients with Alzheimer's disease treated with bapineuzumab: a historical, prospective secondary analysis. *J Neurol Neurosurg Psychiatry*.

[10] Biffi A, Greenberg SM (2011) Cerebral amyloid angiopathy: a systematic review. *J Clin Neurol* **7**, 1-9.

[11] Yates PA, Sirisriro R, Villemagne VL, Farquharson S, Masters CL, Rowe CC, Group AR (2011) Cerebral microhemorrhage and brain beta-amyloid in aging and Alzheimer disease. *Neurology* **77**, 48-54.

[12] Hanyu H, Tanaka Y, Shimizu S, Takasaki M, Abe K (2003) Cerebral microbleeds in Alzheimer's disease. *J Neurol* **250**, 1496-1497.

[13] Carlson C, Estergard W, Oh J, Suhy J, Jack CR, Jr., Siemers E, Barakos J (2011) Prevalence of asymptomatic vasogenic edema in pretreatment Alzheimer's disease study cohorts from phase 3 trials of semagacestat and solanezumab. *Alzheimers Dement* **7**, 396-401.

[14] Black RS, Sperling RA, Safirstein B, Motter RN, Pallay A, Nichols A, Grundman M (2010) A single ascending dose study of bapineuzumab in patients with Alzheimer disease. *Alzheimer Dis Assoc Disord* **24**, 198-203.

[15] Salloway S, Sperling R, Gilman S, Fox NC, Blennow K, Raskind M, Sabbagh M, Honig LS, Doody R, van Dyck CH, Mulnard R, Barakos J, Gregg KM, Liu E, Lieberburg I, Schenk D, Black R, Grundman M, Bapineuzumab 201 Clinical Trial I (2009) A phase 2 multiple ascending dose trial of bapineuzumab in mild to moderate Alzheimer disease. *Neurology* **73**, 2061-2070.

[16] Salloway S, Sperling R, Fox NC, Blennow K, Klunk W, Raskind M, Sabbagh M, Honig LS, Porsteinsson AP, Ferris S, Reichert M, Ketter N, Nejadnik B, Guenzler V, Miloslavsky M, Wang D, Lu Y, Lull J, Tudor IC, Liu E, Grundman M, Yuen E, Black R, Brashear HR, Bapineuzumab, Clinical Trial I (2014) Two phase 3 trials of bapineuzumab in mild-to-moderate Alzheimer's disease. *N Engl J Med* **370**, 322-333.

[17] Barkhof F, Daams M, Scheltens P, Brashear HR, Arrighi HM, Bechten A, Morris K, McGovern M, Wattjes MP (2013) An MRI rating scale for amyloid-related imaging abnormalities with edema or effusion. *AJNR Am J Neuroradiol* **34**, 1550-1555.

[18] Wahlund LO, Barkhof F, Fazekas F, Bronge L, Augustin M, Sjogren M, Wallin A, Ader H, Leys D, Pantoni L, Pasquier F, Erkinjuntti T, Scheltens P, European Task Force on Age-Related White Matter C (2001) A new rating scale for age-related white matter changes applicable to MRI and CT. *Stroke* **32**, 1318-1322.

[19] Bartko JJ (1966) The intraclass correlation coefficient as a measure of reliability. *Psychol Rep* **19**, 3-11.

[20] Hankinson SE, Manson JE, Spiegelman D, Willett WC, Longcope C, Speizer FE (1995) Reproducibility of plasma hormone levels in postmenopausal women over a 2-3-year period. *Cancer Epidemiol Biomarkers Prev* **4**, 649-654.

[21] van Straaten EC, Scheltens P, Barkhof F (2004) MRI and CT in the diagnosis of vascular dementia. *J Neurol Sci* **226**, 9-12.

[22] Sperling RA, Aisen PS, Beckett LA, Bennett DA, Craft S, Fagan AM, Iwatsubo T, Jack CR, Jr., Kaye J, Montine TJ, Park DC, Reiman EM, Rowe CC, Siemers E, Stern Y, Yaffe K, Carrillo MC, Thies B, Morrison-Bogorad M, Wagster MV, Phelps CH (2011) Toward defining the preclinical stages of Alzheimer's disease: recommendations from the National Institute on Aging-Alzheimer's Association workgroups on diagnostic guidelines for Alzheimer's disease. *Alzheimers Dement* **7**, 280-292.

[23] Zago W, Schroeter S, Guido T, Khan K, Seubert P, Yednock T, Schenk D, Gregg KM, Games D, Bard F, Kinney GG (2013) Vascular alterations in PDAPP mice after anti-Abeta immunotherapy: Implications for amyloid-related imaging abnormalities. *Alzheimers Dement* **9**, S105-115.

[24] Doody RS, Thomas RG, Farlow M, Iwatsubo T, Vellas B, Joffe S, Kieburtz K, Raman R, Sun X, Aisen PS, Siemers E, Liu-Seifert H, Mohs R, Alzheimer's Disease Cooperative Study Steering C, Solanezumab Study G (2014) Phase 3 trials of solanezumab for mild-to-moderate Alzheimer's disease. *N Engl J Med* **370**, 311-321.

[25] Ostrowitzki S, Deptula D, Thurfjell L, Barkhof F, Bohrmann B, Brooks DJ, Klunk WE, Ashford E, Yoo K, Xu ZX, Loetscher H, Santarelli L (2012) Mechanism of amyloid removal in patients with Alzheimer disease treated with gantenerumab. *Arch Neurol* **69**, 198-207.

[26] Cordonnier C, Potter GM, Jackson CA, Doubal F, Keir S, Sudlow CL, Wardlaw JM, Al-Shahi Salman R (2009) improving interrater agreement about brain microbleeds: development of the Brain Observer MicroBleed Scale (BOMBS). *Stroke* **40**, 94-99.

[27] Rebeck GW, Reiter JS, Strickland DK, Hyman BT (1993) Apolipoprotein E in sporadic Alzheimer's disease: allelic variation and receptor interactions. *Neuron* **11**, 575-580.

[28] Liu E, Schmidt ME, Margolin R, Sperling R, Koeppe R, Mason NS, Klunk WE, Mathis CA, Salloway S, Fox NC, Hill DL, Les AS, Collins P, Gregg KM, Di J, Lu Y, Tudor IC, Wyman BT, Booth K, Broome S, Yuen E, Grundman M, Brashear HR, Bapineuzumab, Clinical Trial I (2015) Amyloid-beta 11C-PiB-PET imaging results from 2 randomized bapineuzumab phase 3 AD trials. *Neurology* **85**, 692-700.

[29] Wisniewski T, Sigurdsson EM (2010) Murine models of Alzheimer's disease and their use in developing immunotherapies. *Biochim Biophys Acta* **1802**, 847-859.

[30] Van Nostrand WE, Davis J, Previti ML, Xu F (2012) Clearance of amyloid-beta protein deposits in transgenic mice following focal cerebral ischemia. *Neurodegener Dis* **10**, 108-111.

Table 1. Treatment-emergent ARIA-E comparing the incidence proportion of Central Safety Read with Final Read in both APOE ε4 carriers and noncarriers for all intravenous infusions of bapineuzumab and placebo treatment groups

Participant with ARIA-E	APOE ε4 Noncarriers (N=1331)					APOE ε4 Carriers (N=1121)			Grand Total (N=2452)
	Placebo N=524	BAPI 0.5 mg/kg N=337	BAPI 1.0 mg/kg N=329	BAPI 2.0 mg/kg N=141	Noncarrier Total	Placebo N=448	BAPI 0.5 mg/kg N=673	Carrier Total	
MRI Final Read, n(%)	3 (0.6)	19 (5.6)	44 (13.4)	28 (19.9)	94 (7.1)	5 (1.1)	143 (21.2)	148 (13.2)	242 (9.9)
Dosed-through	2/3 (66.7)	10/19 (52.6)	28/44 (63.6)	9/28 (32.1)	49/94 (52.1)	4/5 (80.0)	91/143 (63.6)	95/148 64.2)	-
MRI Safety Read , n(%)	1 (0.2)	14 (4.2)	31[a] (9.4)	20 (14.2)	66 (5.0)	1 (0.2)	103 (15.3)	104 (9.3)	170 (7.0)
Newly identified cases, n(%)	2 (0.4)	5 (1.5)	14 (4.3)	8 (5.7)	29[b] (2.2)	4 (0.9)	44 (6.5)	47[c] (4.2)	76 (3.1)
Missed in Central Safety Read	-	-	-	-	18/29 (62.0)	-	-	33/47 (70.0)	51/76 (67.0)
No Central Safety Read	-	-	-	-	11/29 (38.0)	-	-	14/47 (30.0)	25/76 (33.0)
Not confirmed in Final Read, n	0	1	0	0	1*	0	4	4**	5

* one scan not available to Final Read, ** one not recognized by final readers, 3 downgraded as not ARIA-E or not treatment-emergent, [a] one not ARIA-E per Final Read, [b] 29 cases includes one case not confirmed in Final Read, [c] one scan not available to Final Read was excluded and 3 cases downgraded as not ARIA-E or not treatment-emergent, N= number of enrolled patients, n= subset of sample size, BAPI= bapineuzumab, ARIA-E = amyloid-related imaging abnormalities that include intraparenchymal extravasation of fluid, sulcal effusions and gyral swelling that may or may not be present, an ARIA-E event considered treatment-emergent if it started during or after the first infusion and prior to or on the date of last dose + 137 days, APOE ε4 = apolipoprotein ε4 genotype, incidence proportion is the ratio of the number of participants with the event to the total number of participants * 100.

Table 2 Incidence proportion, and incidence rate per 100 person-years of treatment–emergent ARIA-E cases in both APOE ε4 carriers and noncarriers, (Final MRI Read)

Participant with ARIA-E	APOE ε4 Noncarriers					APOE ε4 Carriers					
						1 and 2 copies of APOE ε4 allele		1 copy of APOE ε4 allele		2 copies of APOE ε4 allele	
	Placebo N=524	BAPI 0.5 mg/kg N=337	BAPI 1.0 mg/kg N=329	BAPI 0.5/1.0 mg/kg N=666	BAPI 2.0 mg/kg N=141	Placebo N=448	BAPI 0.5 mg/kg N=673	Placebo N=337	BAPI 0.5 mg/kg N=508	Placebo N=111	BAPI 0.5 mg/kg N=165
ARIA-E, n	3	19	44	63	28	5	143	4	86	1	57
Incidence proportion, % (95% CI)	0.6 (0.1, 1.7)	5.6 (3.4, 8.7)	13.4 (9.9, 17.5)	9.5 (7.3, 11.9)	19.9 (13.6, 27.4)	1.1 (0.4, 2.6)	21.2 (18.2, 24.5)	1.2 (0.3, 3.0)	16.9 (13.8, 20.5)	0.9 (0.0, 4.9)	34.5 (27.3, 42.3)
Difference Bapi-Placebo, % (95% CI)	-	5.1 (2.3, 7.9)	12.8 (8.8, 16.8)	8.9 (6.4, 11.4)	19.3 (12.2, 26.4)	-	20.1 (16.7, 23.6)	-	15.7 (12.0, 19.4)	-	33.6 (25.4, 41.9)
Incidence rate (95% CI)	0.5 (0.1, 1.5)	5.0 (3.0, 7.8)	12.9 (9.4, 17.3)	8.7 (6.7, 11.2)	19.6 (13.0, 28.3)	0.9 (0.3, 2.2)	20.7 (17.4, 24.3)	1.0 (0.3, 2.6)	15.9 (12.7, 19.6)	0.8 (0.0, 4.2)	38.1 (28.8, 49.3)
Difference Bapi-Placebo, % (95% CI)	-	4.5 (2.6, 6.4)	12.4 (9.4, 15.4)	8.2 (5.8, 10.7)	19.1 (15.3, 22.8)	-	19.7 (15.8, 23.7)	-	14.9 (10.9, 18.9)	-	37.3 (26.7, 47.9)

N= number of enrolled patients, n= subset of sample size, a participant is counted only once regardless of number of episodes, BAPI= bapineuzumab, BAPI= bapineuzumab, CI= confidence interval, ARIA-E = amyloid-related imaging abnormalities that include intraparenchymal extravasation of fluid, sulcal effusions and gyral swelling that may or may not be present, an ARIA-E event considered treatment-emergent if it started during or after the first infusion and prior to or on the date of last dose + 137 days, APOE ε4 = apolipoprotein ε4 genotype, incidence proportion is the ratio of the number of participants with the event to the total number of participants * 100 with the exact binomial 95% CI for the difference in proportions between bapineuzumab and placebo. Incidence rate is the number of participants with an event per 100 person-years at risk. The Poisson exact 95% CI is calculated for each treatment group incidence rate and for the difference.

Table 3 Proportion of participants with first episode of treatment-emergent ARIA-E, and total radiological severity score by bapineuzumab infusion number for APOE ε4 noncarriers and carriers (Final MRI Read)

Number of Infusions Received	APOE ε4 Noncarriers					APOE ε4 Carriers	
	Placebo N=524	BAPI 0.5 mg/kg N=337	BAPI 1.0 mg/kg N=329	BAPI 0.5/1.0 mg/kg N=666	BAPI 2.0 mg/kg N=141	Placebo N=448	BAPI 0.5 mg/kg N=673
1, m/n	1/524	5/337	23/329	28/666	17/141	2/448	39/673
%, 95% CI	0.2 (0.0, 1.1)	1.5 (0.5, 3.4)	7.0 (4.5, 10.3)	4.2 (2.8, 6.0)	12.1 (7.2, 18.6)	0.4 (0.1, 1.6)	5.8 (4.2, 7.8)
Total Radiologic Score Mean (Range)	3.0 (3.0, 3.0)	14.8 (4.0, 46.0)	9.0 (1.0, 56.0)	10.1 (1.0, 56.0)	19.6 (2.0, 57.0)	2.0 (1.0, 3.0)	8.3 (1.0, 52.0)
2, m/n	1/487	8/314	14/308	22/622	8/124	0/426	57/631
%, 95% CI	0.2 (0.0, 1.1)	2.5 (1.1, 5.0)	4.5 (2.5, 7.5)	3.5 (2.2, 5.3)	6.5 (2.8, 12.3)	0.0 (na, na)	9.0 (6.9, 11.5)
Total Radiologic Score Mean (Range)	7.0 (7.0, 7.0)	8.3 (1.0, 24.0)	7.5 (1.0, 23.0)	7.8 (1.0, 24.0)	13.3 (2.0, 25.0)	na	8.6 (1.0, 59.0)
3, m/n	0/440	1/301	4/283	5/584	2/119	2/394	25/589
%, 95% CI	0.0 (na, na)	0.3 (0.0, 1.8)	1.4 (0.4, 3.6)	0.9 (0.3, 2.0)	1.7 (0.2, 5.9)	0.5 (0.1, 1.8)	4.2 (2.8, 6.2)
Total Radiologic Score Mean (Range)	na	17.0 (17.0, 17.0)	5.3 (1.0, 11.0)	7.6 (1.0, 17.0)	5.5 (3.0, 8.0)	2.5 (1.0, 4.0)	6.1 (1.0, 30.0)
4, m/n	1/414	3/278	1/260	4/538	1/112	0/377	10/552
%, 95% CI	0.2 (0.0, 1.3)	1.1 (0.2, 3.1)	0.4 (0.0, 2.1)	0.7 (0.2, 1.9)	0.9 (0.0, 4.9)	0.0 (na, na)	1.8 (0.9, 3.3)
Total Radiologic Score Mean (Range)	2.0 (2.0, 2.0)	4.0 (1.0, 8.0)	1.0 (1.0, 1.0)	3.3 (1.0, 8.0)	1.0 (1.0, 1.0)	na	2.9 (1.0, 5.0)
5, m/n	0/395	1/252	2/241	3/493	0/103	0/360	9/504
%, 95% CI	0.0 (na, na)	0.4 (0.0, 2.2)	0.8 (0.1, 3.0)	0.6 (0.1, 1.8)	0.0 (na, na)	0.0 (na, na)	1.8 (0.8, 3.4)
Total Radiologic Score Mean (Range)	na	5.0 (5.0, 5.0)	8.5 (4.0, 13.0)	7.3 (4.0, 13.0)	na	na	5.7 (1.0, 20.0)
6, m/n	0/367	1/227	0/203	1/430	0/87	1/329	3/422
%, 95% CI	0.0 (na, na)	0.4 (0.0, 2.4)	0.0 (na, na)	0.2 (0.0, 1.3)	0.0 (na, na)	0.3 (0.0, 1.7)	0.7 (0.1, 2.1)
Total Radiologic Score Mean (Range)	na	4.0 (4.0, 4.0)	na	4.0 (4.0, 4.0)	na	1.0 (1.0, 1.0)	5.0 (2.0, 10.0)

N=number of enrolled patients, na = not applicable, CI = confidence interval, BAPI = bapineuzumab, APOE ε4 = apolipoprotein ε4 genotype. Total mean maximum radiologic severity score is the average of the two readers (within a pair of readers) calculated as the sum of the scores of 0 to 5 across 12 regions of the brain for parenchymal and sulcal hyperintensity and swelling, ARIA-E = amyloid-related imaging abnormalities that include intraparenchymal extravasation of fluid, sulcal effusions and gyral swelling that may or may not be present, m is the count of participants with ARIA-E that first occurred on or after the ith infusion and before the (i+1)th infusion, n is the number of participants who have at least i infusions. The exact binomial 95% CI is calculated.

Table 4 Treatment-emergent ARIA-E: time to first occurrence, Kaplan-Meier estimates, and duration of resolved cases for APOE ε4 noncarriers and carriers (Final MRI Read)

Treatment-Emrgent ARIA-E	APOE ε4 Noncarriers					APOE ε4 Carriers	
	Placebo N=524	BAPI 0.5 mg/kg N=337	BAPI 1.0 mg/kg N=329	BAPI 0.5/1.0 mg/kg N=666	BAPI 2.0 mg/kg N=141	Placebo N=448	BAPI 0.5 mg/kg N=673
Time to First Occurrence							
Number of Events (%)	3 (0.6)	19 (5.6)	44 (13.4)	63 (9.5)	28 (19.9)	5 (1.1)	143 (21.2)
Mean (SD)	179 (129.5)	182 (139.4)	112 (94.8)	133 (113.7)	89 (71.6)	215 (188.2)	163 (114.5)
Median, days	178	136	49	131	45	225	134
Range, days	(50, 309)	(41, 497)	(36, 413)	(36, 497)	(29, 308)	(43, 502)	(3, 504)
Kaplan-Meier estimates							
10^{th} percentile (95% CI), days	na (na, na)	na (na, na)	135.0 (48.0, 316.0)	413.0 (141.0, na)	45.0 (41.0, 134.0)	na (na, na)	133.0 (131.0, 135.0)
20^{th} percentile (95% CI), days	na (na, na)	na (na, na)	na (na, na)	na (na, na)	308.0 (120.0, na)	na (na, na)	317.0 (224.0, 500.0)
Duration of Resolved Cases							
Number of Cases	3	10	37	47	20	4	116
Mean (SD), days	110 (73.4)	149 (59.5)	149 (85.8)	149 (80.4)	108 (64.0)	136 (100.6)	166 (97.6)
Median (range), days	97 (44, 189)	141 (88, 234)	108 (49, 390)	108 (49, 390)	91 (11, 274)	92 (72, 286)	129 (32, 457)

Notes: An ARIA-E event is considered treatment-emergent if it started during or after the first infusion and prior to or on the date of last dose + 137 days; The Kaplan-Meier estimates are the 10^{th} and 20^{th} percentile of the length of time to the first occurrence of treatment-emergent ARIA-E; the start of ARIA-E is defined as the date of the first MRI scan on which ARIA-E is identified; the end of ARIA-E is defined as the date of the first MRI scan with no evidence of parenchymal or sulcal hyperintensity or swelling that follows one on which ARIA-E is still or initially identified; duration is imputed as the difference in time from the start to end dates.

Table 5. Prevalence of Hemosiderin deposits <10 mm at baseline for APOE ε4 noncarriers and carriers with and without treatment-emergent ARIA-E (Final MRI Read)

Participants	APOE ε4 Noncarriers					APOE ε4 Carriers	
	Placebo N=524	BAPI 0.5 mg/kg N=337	BAPI 1.0 mg/kg N=329	BAPI 0.5/1.0 mg/kg N=666	BAPI 2.0 mg/kg N=141	Placebo N=448	BAPI 0.5 mg/kg N=673
With presence of HDs (definite or possible) at Baseline, n	87	45	52	97	27	75	120
% (95% CI)	16.6 (13.5, 20.1)	13.4 (9.9, 17.5)	15.8 (12.0, 20.2)	14.6 (12.0, 17.5)	19.1 (13.0, 26.6)	16.7 (13.4, 20.5)	17.8 (15.0, 20.9)
With TE ARIA-E n	2	3	6	9	7	2	38
% (95% CI)	2.3 (0.3, 8.1)	6.7 (1.4, 18.3)	11.5 (4.4, 23.4)	9.3 (4.3, 16.9)	25.9 (11.1, 46.3)	2.7 (0.3, 9.3)	31.7 (23.5, 40.8)
Without TE ARIA-E, n	85	42	46	88	20	73	82
% (95% CI)	97.7 (91.9, 99.7)	93.3 (81.7, 98.6)	88.5 (76.6, 95.6)	90.7 (83.1, 95.7)	74.1 (53.7, 88.9)	97.3 (90.7, 99.7)	68.3 (59.2, 76.5)
Without presence of HDs (definite or possible) at Baseline, n	437	292	277	569	114	373	553
% (95% CI)	83.4 (79.9, 86.5)	86.6 (82.5, 90.1)	84.2 (79.8, 88.0)	85.4 (82.5, 88.0)	80.9 (73.4, 87.0)	83.3 (79.5, 86.6)	82.2 (79.1, 85.0)
With TE ARIA-E, n	1	16	38	54	21	3	105
% (95% CI)	0.2 (0.0, 1.3)	5.5 (3.2, 8.7)	13.7 (9.9, 18.3)	9.5 (7.2, 12.2)	18.4 (11.8, 26.8)	0.8 (0.2, 2.3)	19.0 (15.8, 22.5)
Without TE ARIA-E, n	436	276	239	515	93	370	448
% (95% CI)	99.8 (98.7, 100.0)	94.5 (91.3, 96.8)	86.3 (81.7, 90.1)	90.5 (87.8, 92.8)	81.6 (73.2, 88.2)	99.2 (97.7, 99.8)	81.0 (77.5, 84.2)

N=number of enrolled patients, CI = confidence interval, BAPI = bapineuzumab, APOE ε4 = apolipoprotein ε4 genotype ARIA-E = amyloid-related imaging abnormalities that include intraparenchymal extravasation of fluid, sulcal effusions and gyral swelling that may or may not be present, TE = Treatment-Emergent. An event is considered treatment-emergent if it started during or after the first infusion and prior to or on the date of last dose + 137 days, Total hemosiderin deposits include definite or possible hemosiderin deposits <10 mm or both, incidence proportion is the ratio of the number of participants with the event to the total number of participants in the group * 100. The exact binomial 95% CI is calculated.

Table 6 Proportion of participants with treatment-emergent ARIA-E with first episode of treatment-emergent hemosiderin deposits <10 mm by infusion for all bapineuzumab treatment groups (Final MRI Read)

Number of infusions received	APOE ε4 Noncarriers					APOE ε4 Carriers	
	Placebo N=524	BAPI 0.5 mg/kg N=337	BAPI 1.0 mg/kg N=329	BAPI 0.5/1.0 mg/kg N=666	BAPI 2.0 mg/kg N=141	Placebo N=448	BAPI 0.5 mg/kg N=673
1, m/n	0/3	9/19	9/44	18/63	5/28	0/5	13/143
%, 95% CI	0.0 (na, na)	47.4 (24.4, 71.1)	20.5 (9.8, 35.3)	28.6 (17.9, 41.3)	17.9 (6.1, 36.9)	0.0 (na, na)	9.1 (4.9, 15.0)
2, m/n	0/3	2/17	6/42	8/59	2/19	0/5	23/136
%, 95% CI	0.0 (na, na)	11.8 (1.5, 36.4)	14.3 (5.4, 28.5)	13.6 (6.0, 25.0)	10.5 (1.3, 33.1)	0.0 (na, na)	16.9 (11.0, 24.3)
3, m/n	0/2	1/15	3/38	4/53	2/18	0/4	15/120
%, 95% CI	0.0 (na, na)	6.7 (0.2, 31.9)	7.9 (1.7, 21.4)	7.5 (2.1, 18.2)	11.1 (1.4, 34.7)	0.0 (na, na)	12.5 (7.2, 19.8)
4, m/n	0/2	1/12	0/30	1/42	1/15	0/4	8/105
%, 95% CI	0.0 (na, na)	8.3 (0.2, 38.5)	0.0 (na, na)	2.4 (0.1, 12.6)	6.7 (0.2, 31.9)	0.0 (na, na)	7.6 (3.3, 14.5)
5, m/n	0/2	0/9	1/28	1/37	0/12	0/4	1/88
%, 95% CI	0.0 (na, na)	0.0 (na, na)	3.6 (0.1, 18.3)	2.7 (0.1, 14.2)	0.0 (na, na)	0.0 (na, na)	1.1 (0.0, 6.2)
6, m/n	0/2	0/6	1/9	1/15	0/4	0/3	1/47
%, 95% CI	0.0 (na, na)	0.0 (na, na)	11.1 (0.3, 48.2)	6.7 (0.2, 31.9)	0.0 (na, na)	0.0 (na, na)	2.1 (0.1, 11.3)

N=number of enrolled patients, CI = confidence interval, BAPI = bapineuzumab, na = not applicable, Hemosiderin deposits include definite or possible hemosiderin deposits <10 mm or both, ARIA-E = amyloid related imaging abnormality defined as parenchymal or sulcal hyperintensity or both, and gyral swelling, a finding is considered treatment-emergent if it started during or after the first infusion and prior to or on the date of last dose + 137 days., For recurrent events, only the first event is counted, m is the count of participants with the event that first occurred on or after the ith infusion and before the (i+1)th infusion, n is the number of participants who have at least i infusions. The exact binomial 95% CI is calculated.

Figure 1. MRI Final Read process: sequential, locked individual MRI scan reading performed centrally by pairs of neuroradiologists

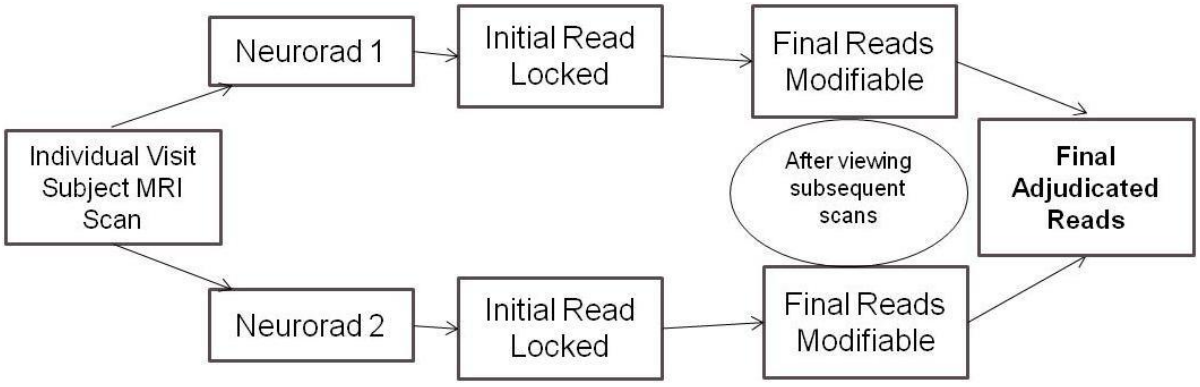

Figure 2. Incidence proportion of ARIA-E for noncarriers with bapineuzumab dose in noncarriers and with copy number of the APOE ε4 allele for participants treated with bapineuzumab 0.5 mg/kg.

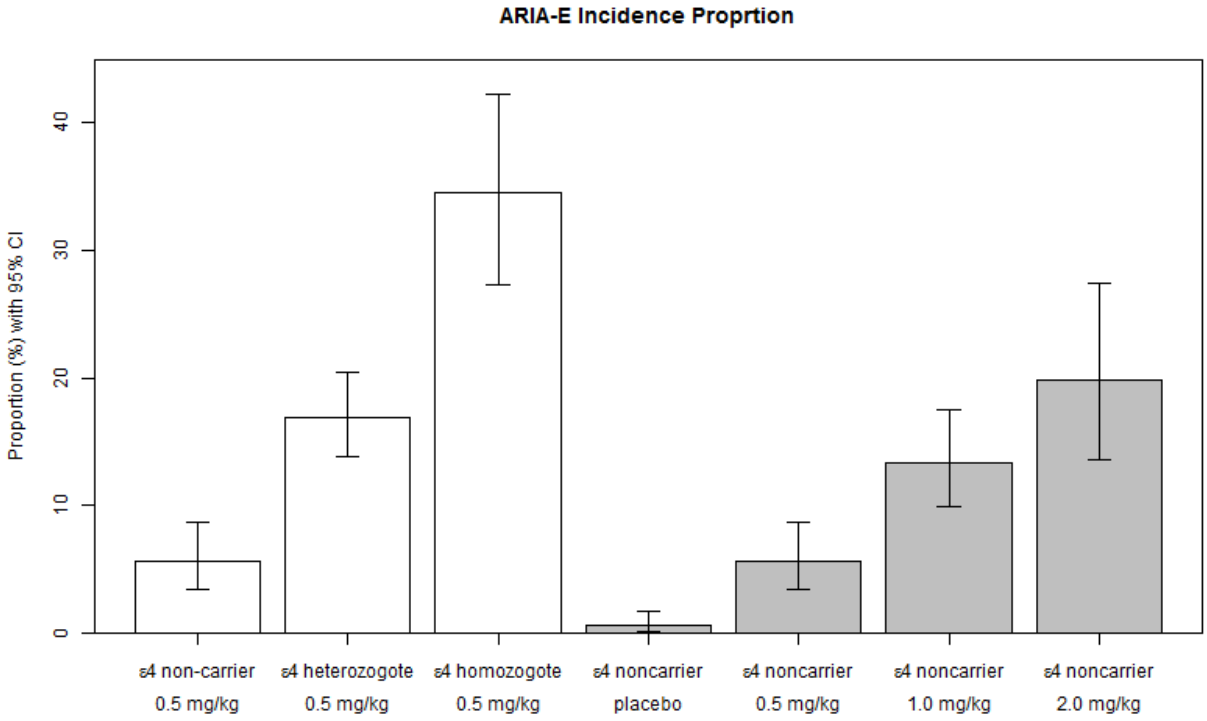

Error bars represent the 95% exact binomial confidence interval

Figure 3. Incidence proportion of first ARIA-E episode by number of bapineuzumab infusions in (A) APOE ε4 noncarriers and (B) carriers.

(A)

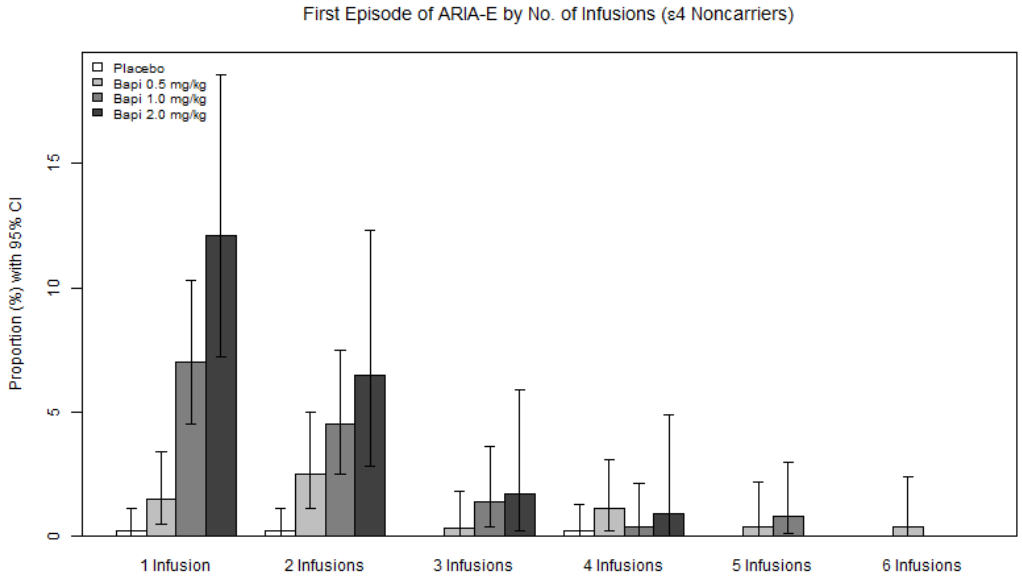

(B)

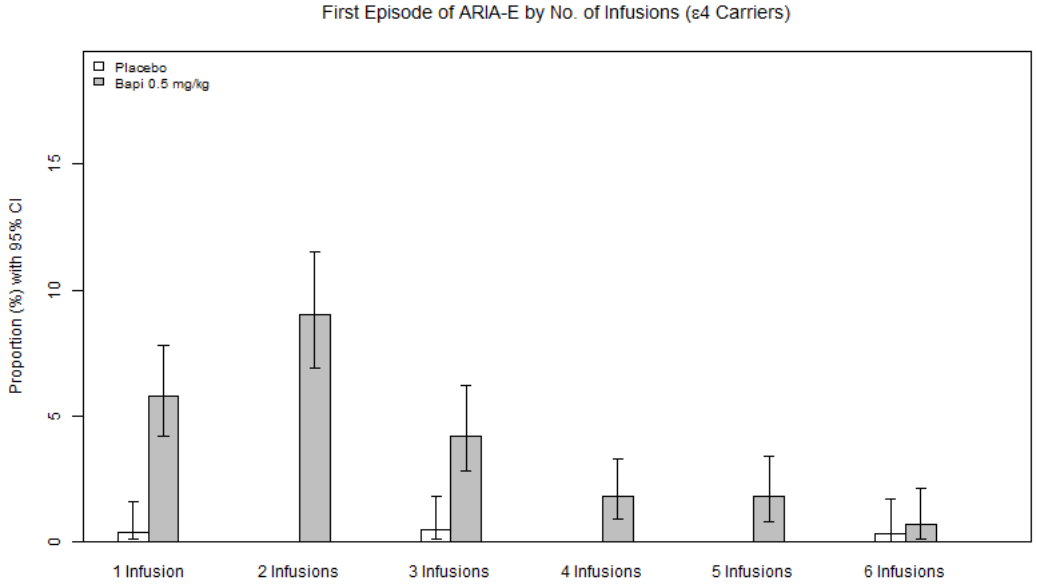

Supplementary Material

MRI acquisition parameters for the three main scanner models at 1.5 Tesla is shown in Table 1S. All MRI images were acquired using a uniform scanning protocol (with respect to: slice thickness, pixel size, pulse sequence, repetition time, echo time, flip angle, number of excitations, etc.) that minimized between-site differences in MRI systems. Each MRI exam consisted of the following MRI sequences: sagittal spin echo (SE), three dimensional (3D) spin-lattice relaxation time (T1) (acquired twice), proton density (PD)/ spin-spin relaxation time (T2), T2* gradient echo (GRE), fluid-attenuated inversion recovery (FLAIR) and diffusion weighted imaging (DWI).

The rules used to compare ARIA-E and ARIA-H Final Read of individual MRI scans made by a pair of independent neuroradiologist for concordance and discordance are provided below in Figures 2S and 3S.

ARIA-E was assessed by location and largest cross-sectional diameter of parenchymal or sulcal hyperintensity, and gyral swelling in each region of the brain (adjudicated by presence or absence, location, and size) [17]. ARIA-H for hemosiderin deposits <10 mm in size (small hemosiderin deposits, microhemorrhage) was assessed by location and number by each region, adjudicated by number (<5 must match, 5-10 higher number, >10 mean number) and location for each of the two types: possible or definite. ARIA-H for hemosiderin deposits ≥10 mm in size (large hemosiderin deposits) was assessed by location and number by each region and adjudicated by number and size. Parenchymal hemorrhage >1 cm in size adjudicated by presence/absence and size. White matter hyperintensity (adjudicated by presence/absence and ARWMC score) by region (frontal, parieto-occipital, temporal, basal ganglia, infratentorial/cerebellum) [18].

Discordance between the two neuroradiologists' assessments was adjudicated by discussion and agreement between the pair to arrive at adjudicated Final Read for that specific MRI scan and the data was analyzed. A summary of adjudication results with respect to extent of concordance and discordance between reader 1 and 2 is shown in Table 2S.

Table 1S. Representative examples of MRI sequence acquisition parameters for 1.5 Tesla MRI scanners in bapineuzumab Phase 3 studies

Sequence/Parameter	2D T1	3DT1	2D PD/T2	2D FLAIR	GRE T2*	2D DWI
Siemens 1.5T						
Acquisition Plane	Sagittal	Sagittal	Axial	Axial	Axial	Axial
Sequence Name	2D Spin Echo	MPRAGE1	2D TSE	2D TIR	2D GRE	2D EPI
TR/TE/TI (ms)	550/14/-	2400/3.6/1000	≥4000/20,120/-	10000/120/2500	420/29/-	5100/137/-
Flip Angle (°)	-	8	-	-	20	-
Matrix (Phase X Frequency)	256 X 256	192 X 256	256 X 256	256 X 256	256 X 256	128 X 128
Phase Encoding Direction	AP	AP	RL	RL	RL	AP
Field of View (mm)	260	240	260	240	240	240
Slice Thickness/Gap (mm)	4/1	1.2/0	3/0	5/1	5/1	5/1.5
Scan Time (minutes: seconds)	1:45	8:00	4:40	3:35	4:30	0:45
Miscellaneous		1Fl3d1_ns 170 slices	Fat Suppression	2 concatenations		B = 1000 (0)
General Electric 1.5T						
Acquisition Plane	Sagittal	Coronal	Oblique/Axial	Oblique/Axial	Oblique/Axial	Oblique/Axial
Sequence Name	2D Spin Echo	3D Fast SPGR	2D FSE	2D T2 FLAIR	2D GRE	2D DW/EPI
TR/TE/TI (ms)	600/14/-	9.4/4.2/450	≥4000/20,120/-	9000/120/2200	550/30/-	11000/81/-
Flip Angle (°)	-	15	-	-	20	-
Matrix (Phase X Frequency)	192 X 256	192 X 192	192 X 256	160 X 256	160 X 256	128 X 128
Frequency Direction	SI	SI	AP	AP	AP	LR
Field of View (mm)	260	240	260	240	240	240
Slice Thickness/Gap (mm)	4/1	1.2/0	3/0	5/1	5/1	5/1.5
Scan Time (minutes: seconds)	1:45	7:35	4:43	3:36	4:32	0:44
Miscellaneous		180 slices	Fat Saturation			B=1000 (0)

Sequence/Parameter	2D T1	3DT1	2D PD/T2	2D FLAIR	GRE T2*	2D DWI
Philips 1.5T						
Acquisition Plane	**Sagittal**	**Sagittal**	**Axial**	**Axial**	**Axial**	**Axial**
Sequence Name	**2D Spin Echo**	**3D TFE**	**2D TSE**	**2D T2 FLAIR**	**2D FFE**	**2D EPI**
TR/TE/TI (ms)	**600/9/-**	**8.6/4.0/1000**	**≥4000/20,120/-**	**10000/120/2500**	**550/30/-**	**Shortest**
Flip Angle (°)	**-**	**8**	**-**	**-**	**20**	**-**
Matrix (Phase X Frequency)	**256 X 256**	**192 X 256**	**256 X 256**	**256 X 256**	**256 X 256**	**128 X 128**
Phase Direction	**AP**	**AP**	**LR**	**LR**	**LR**	**AP**
Field of View (mm)	**260**	**240**	**260**	**240**	**240**	**240**
Slice Thickness/Gap (mm)	**4/1**	**1.2/0**	**3/0**	**5/1**	**5/1**	**5/1.5**
Scan Time (minutes: seconds)	**1:45**	**7:45**	**4:40**	**3:56**	**4:34**	**0:45**
Miscellaneous		**170 slices T1 Enhancement**	**Fat Saturation**	**2 Packages**		**B = 0, 1000**

Notes: MRI scanner manufactured by Siemens (Vision, Symphony or Avanto, General Electric (LX or Excite),Toshiba or Philips Infinion. 2D= two dimensional, 3D=three dimensional, T1= spin-lattice relaxation time, T2=spin-spin relaxation time, PD= proton density, FLAIR= Fluid-attenuated inversion recovery, GRE= gradient-recall echo, DWI=diffusion weighted imaging, TSE=turbo spin echo.

Figure 2S. Annotated consensus rules for adjudication of ARIA-E in individual brain MRI scans performed centrally by a pair neuroradiologist.

SECTION 1: ARIA-E

1a. Is there any evidence of parenchymal hyperintensity?

☐ **Yes** ☐ **No** ☐ **Unable to assess (specify)** _____

For each location, provide a score* for parenchymal hyperintensity on MRI:

☐ Left frontal _____	☐ Right frontal _____
☐ Left temporal _____	☐ Right temporal _____
☐ Left parietal _____	☐ Right parietal _____
☐ Left occipital _____	☐ Right occipital _____
☐ Left Cerebellum/ brainstem _____	☐ Right Cerebellum/ brainstem _____
☐ Left central _____	☐ Right central _____

Compared to previous MRI(s), if available, parenchymal hyperintensity on MRI is:

☐ New ☐ Increased ☐ Unchanged ☐ Partially resolved

1b. Is there any evidence of sulcal hyperintensity?

☐ **Yes** ☐ **No** ☐ **Unable to assess (specify)** _____

For each location, provide score* for sulcal hyperintensity on MRI:

☐ Left frontal _____	☐ Right frontal _____
☐ Left temporal _____	☐ Right temporal _____
☐ Left parietal _____	☐ Right parietal _____
☐ Left occipital _____	☐ Right occipital _____
☐ Left Cerebellum/ brainstem _____	☐ Right Cerebellum/ brainstem _____
☐ Left central _____	☐ Right central _____

Compared to previous MRI(s), if available, sulcal hyperintensity identified on MRI is:

☐ New ☐ Increased ☐ Unchanged ☐ Partially resolved

1c. Is there any evidence of swelling?

☐ **Yes** ☐ **No** ☐ **Unable to assess (specify)** _____

For each location, provide score* for swelling on MRI:

☐ Left frontal _____	☐ Right frontal _____
☐ Left temporal _____	☐ Right temporal _____
☐ Left parietal _____	☐ Right parietal _____
☐ Left occipital _____	☐ Right occipital _____
☐ Left Cerebellum/ brainstem _____	☐ Right Cerebellum/ brainstem _____
☐ Left central _____	☐ Right central _____

Consensus rule notes for parts 1a, 1b and 1c:

1a: Evidence of presence or absence of parenchymal hyperintensity must match exactly, the reason for “unable to assess” does not need to match; radiological severity scores for each brain region must match; comparison to previous MRI(s) must match;

1b: Evidence of presence or absence of sulcal hyperintensity must match exactly, the reason for “unable to assess” does not need to match; radiological severity scores for each brain region must match; comparison to previous MRI(s) must match; and

1c: Evidence of presence or absence of swelling must match exactly, the reason for “unable to assess” does not need to match; radiological severity scores for each brain region must match; comparison to previous MRI(s) must match.

Figure 3S. Annotated consensus rules for adjudication in individual brain MRI scans for ARIA-H (A) hemosiderin deposit(s)<10 mm, and (B) hemosiderin deposit(s) ≥10 mm performed centrally by a pair neuroradiologist

(A)

SECTION 2: HEMOSIDERIN DEPOSIT(S) <10 mm (MICROHEMORRHAGES)

2a. Is there evidence of definite hemosiderin deposit(s) <10 mm (microhemorrhage)?

☐ **Yes** ☐ **No** ☐ **Unable to assess: (specify)**_____

Specify number of definite hemosiderin deposit(s) in each region:

☐ Left frontal # ____	☐ Right frontal #____
☐ Left temporal # ____	☐ Right temporal #____
☐ Left parietal # ____	☐ Right parietal #____
☐ Left occipital # ____	☐ Right occipital #____
☐ Cerebellar gray matter #____	☐ Thalamus # ____
☐ Cerebellar white matter # ____	☐ Brainstem # ____
☐ Other (specify region) _____ # ____	

If yes, specify shape(s) (chose only one box): ☐ Punctate ☐ Linear ☐ Both

2b. Is there evidence of <u>possible</u> hemosiderin deposit(s) <10 mm (microhemorrhage)?

☐ **Yes** ☐ **No** ☐ **Unable to assess: (specify)** _____

Specify number of <u>possible</u> hemosiderin deposit(s) in each region:

☐ Left frontal # ____	☐ Right frontal #____
☐ Left temporal # ____	☐ Right temporal #____
☐ Left parietal # ____	☐ Right parietal #____
☐ Left occipital # ____	☐ Right occipital #____
☐ Cerebellar gray matter #____	☐ Thalamus # ____
☐ Cerebellar white matter # ____	☐ Brainstem # ____
☐ Other (specify region) _____ # ____	

If yes, specify shape(s) (chose only one box): ☐ Punctate ☐ Linear ☐ Both

(B)

SECTION 3: HEMOSIDERIN DEPOSIT(S) ≥10 mm

3a. Are there any hemosiderin deposit(s) ≥10 mm?

☐ **Yes** ☐ **No** ☐ **Unable to assess: (specify)**_____

Specify number of hemosiderin deposit(s) ≥10 mm in each region:

☐ Left frontal #	☐ Right frontal #
☐ Left temporal #	☐ Right temporal #
☐ Left parietal #	☐ Right parietal #
☐ Left occipital #	☐ Right occipital #
☐ Cerebellar gray matter #	☐ Thalamus #
☐ Cerebellar white matter #	☐ Brainstem #
☐ Other: (specify region)	#

Compared to previous MRI, if available, the HD(s) ≥10 mm on this MRI is:

☐ New ☐ Increased in size ☐ Unchanged ☐ Partially resolved

If yes, specify shape(s) (chose all that apply):

☐ **Linear/Curvilinear** ☐ **Other:** _____

Consensus rule notes for parts 2a, 2b, and 3a:

2a and 2b: Evidence of presence or absence of definite or possible hemosiderin deposits <10 mm must match exactly, the reason for "unable to assess" does not need to match; for number of definite or possible HDs if 0 to 5, numbers must match, if 6 to 10: if difference = 1, take the higher number; if difference is >1, then must adjudicate, if >10 , take the average of the 2 numbers; round up to the whole number; any time number falls into 2 categories, use the adjudication rules for the lowest number, for other locations does not need to match.

3a: Presence or absence of HDs ≥10 mm must match exactly, the reason for "unable to assess" does not need to match, numbers must match exactly, but location does not need to match, comparison to previous MRI must match.